ESTIMATION OF LONG PERIOD GROUND MOTIONS BY USING SEMI-EMPIRICAL METHODS

LUO Qifeng[1] and WU Di[2]

[1] *Professor, Shanghai Institute of Disaster Prevention and Relief, Tongji University, Shanghai. China*

[2] *Doctor, Research Institute of Structural Engineering and Disaster Reduction, Tongji University, Shanghai. China*

Email: luo@mail.tongji.edu.cn, wdzooo@sohu.com

ABSTRACT :

In this paper a modified empirical Green's functions (EGF) method is suggested and used for ground motion simulation. The source parameters of asperity and rupture process are decided by the inhomogeneous fault. The synthesis of Tangshan earthquake in far field is used to study the influence of the location of single asperity. Brune's model is used for predicting the Fourier spectrum of single asperity. In order to discover the influence of the aperity parameters on the ground motion, the asperity is simulated in the different conditions, which include the area and the stress drop of the asperity. The simulation result shows that the stress drop and the asperity area play important role in the far field Fourier spectrum. However, the research results show that these source parameters have different influence on the Fourier spectrum at different frequencies.

KEYWORDS: Tangshan earthquake, empirical Green's function, asperity, long-period ground motion, stress drop on the asperity, asperity area

1. INTRODAUCITON

Fifteen earthquakes were listed and analyzed by Somerville et al. (1999). All fifteen of these crustal earthquakes have rupture models in which the slip varies spatially over the fault surface. Many source and asperity parameters of these earthquakes were listed and analyzed by statistics. The asperity studied is defined to enclose fault elements whose slip is 1.5 or more times larger than the average slip over the fault and is subdivided if any row or column has an average slip less than 1.5 times the average slip (Somerville et al., 1999). The relation between the combined area of asperities S_a and seismic moment M_0 determined with constraining the slope to be 2/3 is:

$$S_a(km^2) = 5.00\times10^{-16}\times M_0^{2/3}(\text{dyne}\cdot\text{cm}) \tag{1.1}$$

Source modeling of recent shallow intraslab earthquakes was studied by using strong-motion data by Asano et al. (2003). They maintained that the ratio between the combined area of strong-motion generation areas and the area predicted by the empirical relationship tends to decrease with focal depth. The stress drops on strong motion generation areas (or asperities) of shallow intraslab earthquakes increase with focal depth.

A dynamic model of a single, isolated asperity was used as a simulation for a small aftershock of 1975 Oroville earthquake by Das and Boatwright (1985). The acceleration waveforms and envelopes from a small aftershock were modeled by the failure of an asperity. By comparison, the continuing acceleration which follows the asperity failure process cannot be modeled exactly by using the method which assumes no further stress drop occurs during the equilibration of slip outside the asperity.The simpler problem of radiation from the fracturing of a circular asperity at the center of a circular fault was studied by Das and Kostrove (1986).Preliminary evidence suggests that the average stress drop on the asperity is increased by a certain ratio over the average stress drop that had previously occurred over the annular region of the fault. A static model for asperities were put forward by assuming that motion on the fault is resisted primarily by a patch of small strong asperities that interact with each other to increase the amount of displacement needed to cause failure by Johnson and Nadeau (2002). This asperity patch is surrounded by a much weaker fault that continually creeps in response to tectonic stress. They assumed that the moment release is triggered by the failure of the strong asperity patch and most of the moment comes from the displacement shadow. The assumption is that the stress drop on the none-asperity is zero when the asperities fail in this method. Were all of the asperities to rupture and the displacement deficit released, they get the scalar moment M_a of such an event would be

$$M_a = 4\mu D_a r_a R \tag{1.2}$$

Where r_a is the radius of the strong asperity patch, R is the outer radius of the displacement shadow, μ is the shear modulus.

An asperity was defined as a region in which the slip is larger by a prescribed amount than the average slip over the fault surface (Johnson and Nadeau, 2002). Based on the earthquakes researched by Somerville et al. (1999), Wu (2008) get the average stress drops on all the asperities by statistics based on 15 earthquakes. The average stress drop on the asperities is

$$\Delta\sigma_a \approx 140\,bar \tag{1.3}$$

2. THE INFLUENCE OF THE RELATIVE LOCATION OF THE ASPERITY ON THE FAULT ON THE FAR FIELD RESPONSE SPECTRUM

Firstly, the main shock fault plane is divided into asperity area and non-asperity area. The stress drop on the asperity is assumed to be the average stress proposed by equation (1.3). And the asperity area is divided into small cells. The non-asperity area also can be divided into small non-asperity cells.

A modified empirical Green's functions (EGF) method is suggested by Wu (2008), in which the asperity cells have same stress. The record of small aftershock is needed to modify into that radiated from the small asperity cell and the small non-asperity cell. Each small cell will produce the wave when the propagating rupture reaches the cell. So that the ground motions of main shock can be synthesized by the waves radiated from the asperity cells and non-asperity cells as follows,

$$u(t)=\sum_{i=1}^{N_l}\sum_{j=1}^{N_w}u_{nij}(t-t_{nrij}-t_{ncij})+\sum_{k=1}^{N_{al}}\sum_{m=1}^{N_{aw}}u_{akm}(t-t_{arkm}-t_{ackm}) \tag{2.1}$$

Where, $t_{arkm}=\left|\xi_0-\xi_{akm}\right|/V_r$ and $t_{ackm}=\left|\mathrm{R_s}-\mathrm{R_{akm}}\right|/\mathrm{V_c}$ denote the time delay for the rupture propagation and the wave propagation of the (*k, m*) asperity cell, $t_{nrij}=\left|\xi_0-\xi_{nij}\right|/V_r$ and $\mathrm{t_{ncij}}=\left|\mathrm{R_s}-\mathrm{R_{nij}}\right|/\mathrm{V_c}$ denote the time delay for the rupture propagation and the wave propagation of the (*i, j*) non-asperity cell. ξ_0, ξ_{akm} and ξ_{nij} denote the coordinate of the rupture beginning location in main shock, the (*k, m*) asperity cell and the (*i,j*) none-asperity cell. $\mathrm{V_r}$ and $\mathrm{V_c}$ denote the velocity of rupture on the fault and wave propagation. R_s, R_{akm} and R_{nij} denote the source distance of the aftershock, the distance from the (*k, m*) asperity cell to the receiver and from the (*i, j*) none-asperity cell to the receiver.

The Tangshan earthquake is considered as two sub-faults which consists of southern sub-faults striking N30°E and northern sub-faults strikes N50°E in the simulation (Zhou, 1985) (Luo and Hu, 1997). The main shock epicenter is located at the southern part. The sub-faults are shown in Table 2.1 in detail.

Table 2.1 The sub-fault parameters of Tangshan earthquake

Sub-fault	Strike $\phi(^\circ)$	Dip $\delta(^\circ)$	Rake (km)	M_0 $(dyne\cdot cm)$	$L\times W$ $(\mathrm{km^2})$	$\Delta\sigma$ (bar)	$\overline{D}$ (cm)
1	30	80	180	7.1×10^{26}	57×20	20	186
2	50	80	180	6.9×10^{26}	57×20	19	186

The seismic parameters of the main shock were determined by some reports mentioned above. The μ and the quality factor Q are considered as $3.3\times10^{10}N/m^2$ and 500, respectively.

The records of the Ninghe earthquake (MS = 6. 9) are chosen as Green function to synthesize the far-field accelerations of the main shock. The parameters of the aftershock are shown in Table 2.2 in detail.

Table 2.2 The parameters of Ninghe earthquake

Epicentre	Depth (km)	strike	Dip	M_0 $(dyne\cdot cm)$	$L\times W$ $(\mathrm{km^2})$	$\Delta\sigma$ (bar)	$\overline{D}$ (cm)
$39^\circ17'N\quad118^\circ47'E$	17	330°	39°	8.0×10^{25}	18×9	35	149.6

The Tangshan earthquake and the Ninghe earthquake were recorded at Guanting station. The epicentral distance

of the main shock at Guanting station is 228 *km*, and the epicentral distance of the Ninghe earthquake at Guanting station is 216 *km*. For all the asperities, the relation between the asperity area A_a and the fault A is proposed by Somerville et al. (1999). The approximately asperity area A_a is given by

$$A_a = 0.22 \times A \tag{2.2}$$

In order to show the influence of relative location of the single asperity, the 22 percent of the fault area of Tangshan earthquake is taken as the single asperity. Several main shock models with single asperity in different location are considered, and the different locations of asperities are shown in Figure1.

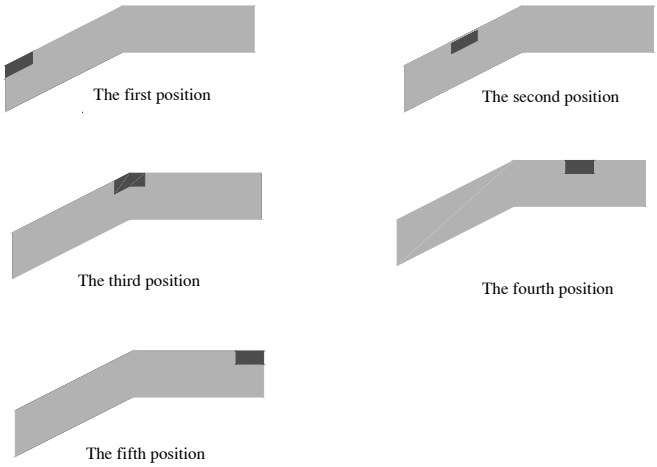

Figure 1 Five different locations on Tangshan earthquake fault

The rupture is assumed to start from right side of the fault, and rupture direction is from right to left. Figure 2 shows the response spectra (NW component) of the synthesized accelerations of the main shock at Guanting station. The response spectrum of observed Tanshan seismic acceleration is given out in Figure 2.

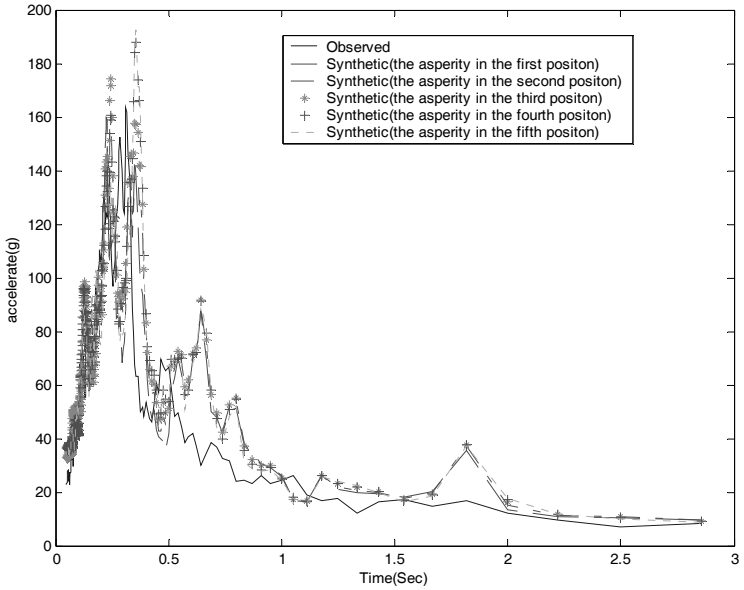

Figure 2 Comparison of response spectra of five synthesized accelerations with different asperity locations on the fault

Figure 3 shows that the synthetic response spectra have the same decay relationship in far field, and they

are consistent with the response spectrum of observed record. It can be seen that the locations of asperity have large influence on response spectra in the period range from 0.2 to 0.4 second. The maximum values of response spectra decrease with the location which moving along the strike direction of the fault. And the peak value of response spectrum reaches the maximum when the single asperity is located at the rupture end of the fault. The locations of the asperities on the fault have less influence on response spectra in long period range.

3. INFLUENCE OF ASPERITY PRAMETERS ON THE FOURIER SPECTRUM

To demonstrate how these parameters of the single asperity influence the far field response spectrum in actual earthquakes, the single asperity is taken as target for research. The circular single asperity was studied by using earthquake source model proposed by Brune(1970) in this paper, and the relationship between the stress drop on the asperity, the seismic moment of asperity, the combined asperity area is also researched. This Brune's model describes near- and far-field displacement spectra and includes the effect of fractional stress drop. The modified far-field S wave amplitude spectrum $F_a(\omega)$ of an asperity can be described by (Wu, 2008)

$$F_a(\omega) = R(\theta,\Phi)\frac{r_a}{R}\frac{\Delta\sigma_a}{\mu}\beta\frac{1}{(\omega_{ca}+i\omega)^2}(1-\frac{2\pi}{Q})^{\omega R/4\pi\beta} \tag{3.1}$$

Here, $R(\theta,\Phi)$ is the radiation pattern , R is the hypocentral distance and taken as 228km, $\Delta\sigma_a$ is the stress drop on the asperity, ω_{ca} is the corner frequency, r_a is the equivalent radius of single asperity given by $r_a = \sqrt{S_a/\pi}$, where β is the shear wave velocity and taken as 3. 3 *km/s*, i is an imaginary unit, Q is the quality factor and taken as 500. In order to compare the synthetic model with Tangshan earthquake, some Tangshan seismic parameters have been adopted in the formula.

3.1. Influence of the Asperity Area on the Far Field Fourier Amplitude Spectrum with the Same Stress Drop on the Asperity

In Brume's model the corner frequency ω_{ca} is given by

$$\omega_{ca} = 2.34\beta / r_a \tag{3.2}$$

Then equation (3.1) can be written as

$$F_a(\omega) = R(\theta,\Phi)\frac{\sqrt{S_a/\pi}}{R}\frac{\Delta\sigma_a}{\mu}\beta\frac{1}{(2.34\beta\sqrt{\pi/S_a}+i\omega)^2}(1-\frac{2\pi}{Q})^{\omega R/4\pi\beta} \tag{3.3}$$

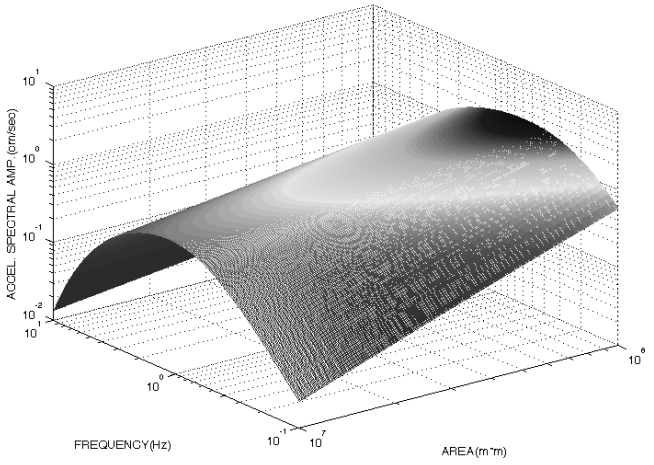

Figure 3 The Fourier amplitude spectrum of single asperity with the increasing of the asperity area from 10 to 100 km^2 and the constant Stress Drop on the Asperity

The stress drop on the asperity is taken as 140 bar and the asperity area increases from 10 to 100 km^2, the calculated Fourier spectrum is shown in figure 3. Figure 3 shows that when the stress drop is kept constant, the Fourier amplitude spectrum increases rapidly with the increased area of single asperity from 10 to 100 km^2. The Fourier amplitude spectrum increases obviously faster in low frequency range than in high frequency range. It means that the asperity area is a very important factor which affects the Fourier amplitude spectrum.

3.2. Influence of the Stress Drop on the Asperity on the Far Field Fourier Amplitude Spectrum with the Same Asperity Area

Assume the asperity area is 10 km^2 and the stress drop of single asperity increases from 10 to 200 bar. The calculated Fourier amplitude spectra with frequencies are shown in figure 4.

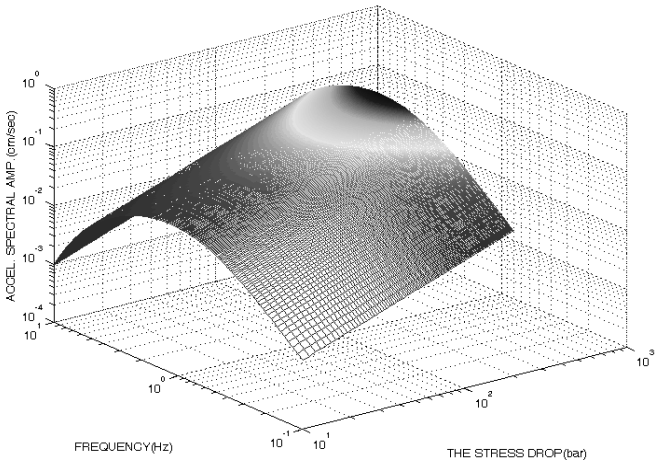

Figure 4 The Fourier amplitude spectrum of single asperity in far field with the variation of the stress drop on the asperity and the constant asperity area

From figure4 we can conclude that when the asperity area is invariant the Fourier amplitude spectra increased obviously with the increase of stress drop on the single asperity. And the shapes of spectrum are approximately the same in all frequencies. This suggests that the stress drop on the asperity is a very important factor which affects the Fourier amplitude spectrum in all frequencies.

3.3. Influence of the Stress Drop on the Single Asperity on the Far Field Fourier Amplitude Spectrum with the Same Seismic Moment of Asperity

Seismic moment M is commonly calculated using the formula proposed by Kanamori and Anderson (1975)

$$M = 16/7 * \Delta\sigma * r^3 \tag{3.4}$$

Where $\Delta\sigma$ is the mean stress drop over a circular crack of radius r. For a single circular asperity-source model, using $\Delta\sigma_a$ for $\Delta\sigma$ and r_a for r yields

$$M_a = 16/7 * \Delta\sigma_a * r_a^3 \tag{3.5}$$

From equation (3.5) we have

$$r_a = 0.76(M_a / \Delta\sigma_a)^{1/3} \tag{3.6}$$

And then equation (3.1) can be written

$$F_a(\omega) = 0.76R(\theta,\Phi)\frac{M_a^{1/3}}{R}\frac{\Delta\sigma_a^{2/3}}{\mu}\beta\frac{1}{(3.08\beta(\Delta\sigma_a/M_0)^{1/3}+i\omega)^2}(1-\frac{2\pi}{Q})^{\omega R/4\pi\beta} \tag{3.7}$$

The Fourier amplitude spectra are shown in figure 5 with the stress drop on the single asperity increasing from

10 to 400 bar. In this cases, the seismic moment of asperity is $1\times10^{18}N\cdot m$.

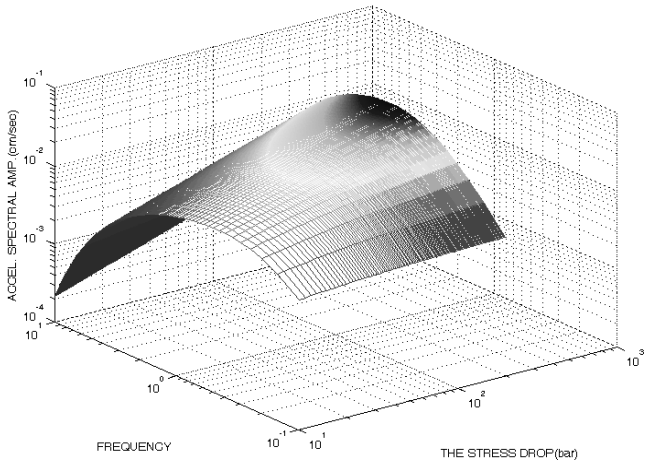

Figure 5. The Fourier amplitude spectrum of single asperity in far field with the variation of the stress drop on the asperity and the constant seismic moment

From figure 5 we can know that the Fourier amplitude spectrum in high frequency is increased faster than in low frequency when the stress drop on the single asperity increased from 10 to 400 bar and the seismic moment of asperity kept constantly. The spectrum is almost unchanged when frequency is near the 0.1 Hz.
If the seismic moment of asperity keeps invariant, the increase of the stress drop on single asperity means the decrease of the asperity area. When the asperity area decreased, the spectrum in high frequency decreased more slowly than the spectrum in low frequency. However, the increase in Fourier amplitude spectra is similar at different frequencies with the increase of stress drop on the asperity. So the result accords with the conclusion. And the stress drop on asperity plays more important role than the asperity area.

3.4. Influence of the Area of Single Asperity on the Far Field Fourier Amplitude Spectrum with the Same Seismic Moment of Asperity

Assume the asperity is circular with radius r_a and area $S_a=\pi r_a^2$. Then equation (3.4) can be written

$$\Delta\sigma_a = 2.43\,M_a S_a^{-3/2} \tag{3.8}$$

The Fourier amplitude spectrum of single asperity in far field becomes

$$F_a(\omega)=1.37R(\theta,\Phi)\frac{M_a\beta}{S_aR\mu}\frac{1}{(2.34\beta\sqrt{\pi/S_a}+i\omega)^2}(1-\frac{2\pi}{Q})^{\omega R/4\pi\beta} \tag{3.9}$$

The variation of Fourier amplitude spectra are shown in figure 6 with the area of single asperity increasing from 10 to $100\,km^2$. The seismic moment of asperity is $1\times10^{18}N\cdot m$.

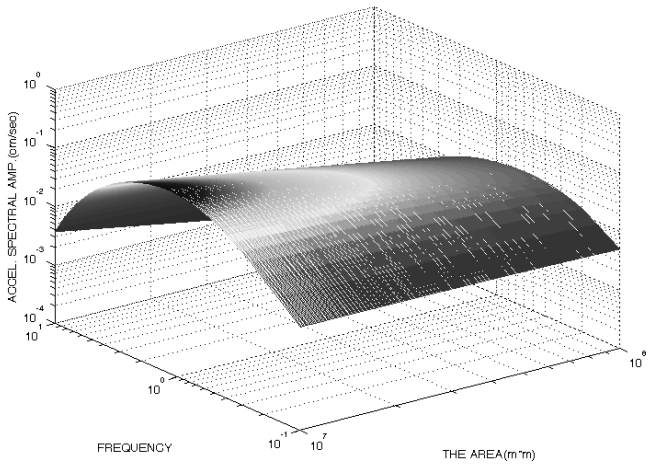

Figure 6 The Fourier amplitude spectrum of single asperity in far field with the variation of the asperity area and the constant seismic moment

From figure 6 we can see that the Fourier amplitude spectrum is not changed obviously in low frequency, while it is decreased in high frequency with the area of single asperity increased from 10 to 100 km^2 when the seismic moment of is kept the same. The conclusion can be get that area of asperity can hardly affect the Fourier amplitude spectrum in low frequency in far field when the seismic moment of asperity remains constant. Consequently, the increasing of asperity area can reduce the Fourier amplitude spectrum in high frequency.

4. CONCLUSIONS

The spectra of fault model with single asperity in different location on the fault have been simulated based on the empirical Green's functions method. Also the Fourier spectrum radiated from a single asperity is calculated by using the Brune's model. Some conclusions could be reached from the simulated the Fourier amplitude spectrum of the single asperity.

1. The location of asperity has larger influence on response spectra in short period range than in long period range. The maximum values of response spectra decrease with the location which moving along the strike direction of the fault and the peak value reaches the maximum when the asperity locates at the rupture end of the fault.

2. The Fourier amplitude spectra in different frequencies are increased with the expansion of the asperity area, and the asperity area has great influences on spectrum in low frequency range than in high frequency range.

3. The Fourier amplitude spectra increase obviously with the increase of stress drop on asperity. Also, the shape of spectrum can hardly be affected by stress drop on asperity in all the frequencies.

4. When the seismic moment of asperity keeps invariant, the stress drop on single asperity plays a decisive role in the Fourier amplitude spectrum.

REFERENCES

Somerville P, Ikula K, Graves R, et al. . (1999). Characterizing crustal earthquake slip models for the prediction of strong ground motion. *Seismological Research Letters* **70:1,** 59-80.

Asano K, Iwata T and Irikura K. (2003).Source characteristics of shallow intraslab earthquakes derived from strong-motion simulations. *Earth Planets Space*, **55,** 5–8.

Das S and Boatwright J. (1985).The breaking of a single asperity: Analysis of an aftershock of the 1975 Oroville, California, earthquake, *Bull. Seim. Soc. Am.*,**75:3,** 677-687.

Das S and Kostrov B V. (1986). "Fracture of a single asperity on a finite fault: A model for weak earthquakes?" in Earthquake Source Mechanics, American Geophysical Union, Washington, D.C.

Johnson L R and Nadeau R M. (2002). Asperity model of an earthquake: static problem, *Bull. Seim. Soc. Am.* **92:2,** 672–686.

Wu D. (2008). Synthesis and estimation of long period ground motions in far field and the characteristic of crustal seismic slip. Doctoral Dissertation, Tongji, published by Tongji University,Shanghai

Zhou H L. (1985). Some characteristics of source processes of large shallow strike-slip earthquakes, *Acta Geophsica Sinica*, **28:6,** 579-587 (in Chinese)

Luo Q F and Hu Y X. (1997). Synthesis of accelerations of the 1976 Tangshan earthquake (MS 7.8) in near- and far-field by using semi-empirical method. *Acta Seismologica Sinica*, **210:3,**347-354.

Brune J N. (1970). Tectonic stress and the spectra of seismic shear waves from earthquakes. *J Geophys Res*, **75,26,** 4997-5009.

Kanamori H and Anderson D L. (1975). Theoretical basis of some empirical relations in seismology. *Bull. Seim. Soc. Am.*, **65:5,** 1073 - 1095.